International Journal of Modern Studies in Mechanical Engineering (IJMSME)
Volume 1, Issue 1, June 2015, PP 27-44
www.arcjournals.org

The Effect of Local Fuel/Air Ratio on the Performance and Pollutant Emission Formation of a Compression Ignition Engine

Gerald J. Micklow, Ph.D, PE[1], David Becknell[2], Ehsan Tootoonchi[3], Helge von Helldorff[4], Darren Levine[5]

Florida Institute of Technology
Department of Mechanical and Aerospace Engineering
Melbourne, FL USA

Abstract: *The desired product composition and thermodynamic properties produced by a closed combustion chamber is heavily influenced by reactant distribution and ignition source. A fundamental and defining mechanism behind these reaction properties is the burn rate which is a strong function of local equivalence ratio gradient and vaporous fuel concentration when ignition conditions are reached. The ignition source location and the ensuing combustion process rely on the vaporous fuel concentration at local volumes of high energy gradient within the combustion chamber.*

Desirable operation characteristics for internal combustion engines, such as low temperature of combustion to achieve low NO production are often reached at lean local and/or lean global equivalence ratios. As a result, advanced fuel injection systems and combustion chamber design attempt to maintain a stable reaction at the edge of the lean blowout limit. The study performed here presents a comprehensive analysis of the effect of equivalence ratio gradient and concentration properties to enable a stable lean burn to improve engine efficiency and lower pollutant emissions.

The parametric study utilizes the KIVA3 code to investigate the effect of nozzle geometry, fuel injection timing and duration to control the local equivalence ratios to maximize engine efficiency while minimizing nitrogen oxide pollutant emissions. It concludes that through varying fuel injection start and duration and currently available cost effective technologies to produce nozzles with an increase in number of fuel injection holes, emissions can be reduced while still preserving or increasing power and efficiency.

Keywords: *Fuel/Air ratio, equivalence ratio, KIVA3V, combustion, fuel injection, fuel spray, compression ignition, pollutant emissions, efficiency*.

Nomenclature

A	Arrhenius pre-exponential factor
c_f	ensemble averaged concentration of fuel
c_{O2}	ensemble averaged of fuel oxygen
c_p	ensemble averaged concentration of products
E_a	Activation Energy
k	turbulent kinetic energy
n_i	stoichiometric coefficient
P	Pressure
RR	Reaction Rate
r_f	stoichiometric oxygen requirement to burn 1 kg fuel
T	Temperature
U	velocity
ε	Rate of dissipation of turbulent kinetic energy
ν	kinematic viscosity of fuel, cm^2/sec
ρ	density

Subscripts

a *air*

f *fuel*

0 outlet

ATDC After Top Dead Center

BTDC Before Top Dead Center

CA Crank Angle

TPI fuel injection temperature

IMEP Indicated Mean Effective Pressure

1. INTRODUCTION

Today, our nation faces tremendous energy, economic and environmental challenges. Significant changes in the production and consumption of energy must take place to minimize adverse energy and environmental impacts. Currently, a large portion of the energy consumed in the US comes from non-renewable fossil and nuclear fuel. Transportation accounts the majority of the petroleum consumed and the transportation sector is highly dependent on oil. Further, with a steady increase in the number of vehicles and miles traveled, air quality problems in our cities continue to worsen. It is now recognized that one of the "clean" products of complete combustion, CO_2, is a strong contributor to the greenhouse effect, and may ultimately be the most dangerous by-product. Global fuel conservation and a reduction of our reliance on foreign oil supplies as well as environmental concerns are compelling reasons to find cost-effective solutions to reduce our consumption of energy. Since the automobile forms an important component of the U.S. economy, and is an integral part of our lives, it is essential to address the issues of increased fuel efficiency and reduced pollutant emissions. Such a solution would have a positive impact on the environmental issues and lessen our reliance on foreign oil supplies.

To accomplish these tasks, in 1993, industry and government outlined a ten-year program entitled the Partnership for a New Generation Vehicle (PNGV) [1]. The partnership pursued substantial advances in vehicle technology that led to marked improvements in fuel efficiency and emissions of standard vehicle designs. The primary goal was the attainment of three times the fuel efficiency (80 mpg) of today's six passenger family sedan without sacrificing cost, comfort or power. One of the most important improvements required to obtain these goals was to have an engine thermal efficiency in the range of 45-55 percent. The direct injection compression ignition engine was selected as the only engine that could approach this requirement in the near future.

Four-stroke, compression-ignition direct injection (CIDI) engines offer a potentially desirable alternative to conventional SI engines with thermal efficiencies that may approach 40 percent. The fundamental advantage of the diesel engine lies in the direct link between the mixture preparation and auto-ignition. The thermodynamic condition of the mixture necessary for auto-ignition can always be reached with a sufficient compression ratio. Ignition will take place in any region of the inhomogeneous mixture where sufficient conditions for combustion exist. With their non-homogeneous combustion process, direct-injection diesel (compression ignition) engines allow overall leaner combustion, resulting in higher baseline efficiency (about 40 percent peak), 20 to 35 percent better fuel economy, 10 to 20 percent lower CO_2 emissions, near-zero evaporative emissions, and low cold-start emissions. Current designs of diesel engines, however, still produce unacceptable levels of nitrogen oxide (NO) and particulate emissions (mainly soot) at high engine loads. To accomplish the goal of using the diesel cycle in an alternative high-efficiency engine, research is required in the areas of fuel injection, in-cylinder fuel distribution, combustion, temperature distribution, and pollutant emission formulation.

The diesel engine represents one of the more complex combustion systems used today; consequently, understanding the physics and chemistry involved in diesel combustion is quite challenging. Specifically, the major complexity of diesel engines arises due to transient effects and the in homogeneity of spray combustion. An overall description of diesel combustion requires an understanding of three major processes: spray dynamics and the interaction with the combustion chamber walls, ignition kinetics and post-ignition combustion. Computational techniques are continuing to provide improvements in predictive insight into the combustion processes, and are utilized in this work to calculate the appropriate physical phenomenon occurring within an internal combustion engine. The proposed study

will consist of a computational investigation to address these issues for spray combustion. Analysis of multi-hole injection spray fuel injectors has shown that an increased velocity gradient at the nozzle entrance promotes liquid jet breakup [2] which will directly affect the homogeneity of the fuel-air mixture. A method that shows promise for emission reduction with potential gains in efficiency is the modification of local equivalence ratio gradients within the combustion chamber volume [3]-[5]. This is accomplished through the adjustment of fuel sprays and injection methods, which has the potential to reduce harmful emissions without significant efficiency or power losses.

Computational and experimental studies found in literature indicate that beneficial emission modifications can be achieved through the development of injector technologies that produce smoother initial fuel dispersion gradients throughout the cylinder, promoting a more instantaneous burn [6],[7]. Advances in compression ignition engine injection technologies within the class of large industrial combustion engines can be easily applied to medium and small compression ignition engine uses, such as over the road trucking and light vehicle applications [7].

To analyze such hypothesis through computational studies, the Caterpillar 3406 was chosen as a test bed engine model for this paper. The Caterpillar 3406 engine currently employs a six hole fuel injector in each cylinder for the baseline case. An eight hole injector was also studied. At the time of manufacture for these fuel injectors, technology limited hole diameter to approximately 220 microns but today through the use of lasers, water jets, and EDM technology, holes as small as 150 microns in diameter can be manufactured. By using these new manufacturing technologies, fuel spray patterns within the cylinder can be produced to reduce local equivalence ratio gradients, increase overall burn rate, and decrease harmful NO emissions [7].

Using a combination of injection timing and duration optimization, as well as modifications to the injection distribution pattern, the work in this paper aims to provide case studies for which engineering applications can produce fuel distributions reaching greater levels of homogeneity within the combustion chamber volume at lean equivalence ratios, increasing burn rate and stability, while decreasing emission production. This work investigates the effects of varying equivalence ratio, injector timing, and injection duration on emission and power production in a Caterpillar 3406 compression ignition engine.

The current computational study activities will use the KIVA-3V [8] computer code. The spray modeling in KIVA-3V is based on a discrete particle technique [9], in which computational particles are injected into the domain. Each computational particle contains a number of droplets of identical size, velocity and temperature. Probability distributions govern the assignment of droplet properties at injection using a Monte Carlo sampling technique [10], [11].The particles and fluid interact by exchanging mass, momentum and energy. Modeling the droplet collisions and coalescence [10]is included using an aerodynamic Taylor Analogy Breakup Model[12].The location, shape, rate of development, and mass flow distribution within each fuel jet are of paramount importance in controlling fuel air mixing, wall interactions, combustion rate and the resulting levels of emissions.

Similar ongoing investigations [13], [14] have found that the accurate modeling of the liquid spray must be obtained to study overall engine performance and pollutant emission formation. If the in-cylinder liquid and vaporous fuel distribution is incorrectly modeled, then the resulting combustion process and temperature distribution will be inaccurate and the pollutant emission predictions will be of little or no value. The fuel injection model will be discussed in greater detail in a following section.

The most recent version of the KIVA-3V code has been modified with improved physical models in previous studies. These include the effects of an improved spray model to provide the correct fuel spray penetration and distribution within the cylinder, a fuel spray-wall impingement model, an improved heat transfer model, a mixing-controlled hybrid turbulent combustion model [15] and a soot formation model[16]. The code modifications were validated against available experimental data and good agreement was found for a Caterpillar 3406 compression ignition engine under actual operating conditions. These previous simulation results are shown in Fig for the average in-cylinder pressure [16]. It is seen that excellent agreement is obtained between the measured and computational results. Numerous different run conditions were compared with similar agreement and can be found in the work of Gong [17].

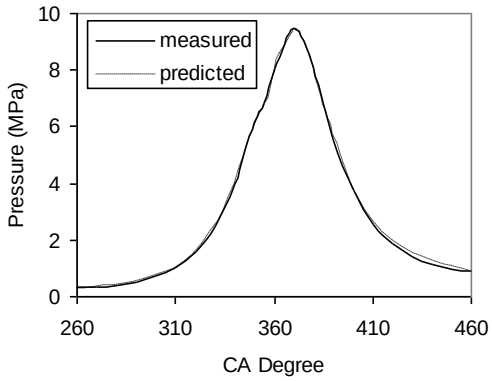

Fig1. *Comparisons of measured and computed cylinder pressure for baseline engine case at 1600 rpm and 75% load.*

2. NUMERICAL DETAILS

The current computational analysis is carried out using the computer code KIVA-3V. KIVA-3V code[8] is one of the recent versions of a series of codes that were developed over the last 25 years at Los Alamos National Laboratory. The code's primary application is the modeling of the complex combustion processes in internal combustion and gas turbine engines. Predecessors to KIVA-3V, i.e., KIVA-III, KIVA-II, and KIVA have been widely used by the automobile industry for a number of years and have been thoroughly tested under a wide range of operating conditions. The KIVA-3V computer code is a version of the KIVA series of codes that solves the compressible, turbulent, three-dimensional transient equations of multi-component gas mixtures with the flow dynamics of an evaporating liquid spray with the capability to handle moving valves[18]. The conservation laws for vapor-gas mass, momentum and energy are solved by a Lagrange-Euler finite volume approach by using an explicit time marching technique. KIVA-3V uses an explicit quasi-second order upwind scheme for convection. This scheme is monotone and approaches second order accuracy when convecting smooth profiles. Typically, turbulence is modeled using a standard isotropic k-ε model. While this may work for a large class of flow fields, it has been found to be inadequate for the flows past intake valves where large vortical structures are formed. Improvements are found by using a Re-Normalization Group (RNG) theory k-ε that improves the accuracy of simulation for flows with large vortical structures such as flows past intake valves. Although accuracy is improved, computational effort is increased relative to the standard model.

3. COMBUSTION MODELING

Detailed mechanisms and rate coefficients for chemical reactions of practical interest are often highly uncertain, so multidimensional reactive flow calculations ordinarily use simplified "global" chemical kinetics schemes, in which the reaction of interest is represented by a manageably small number of reaction steps involving a small number of chemical species [19].

Overall kinetic schemes attempt to simplify the chemistry to predict important physical quantities while maintaining computational efficiency. These quantities are rate of heat release, in-cylinder pressure and temperature, and the concentration of important principal species, fuel, CO, CO_2, H_2, and H_2O. The combustion model used in this study was developed by Micklow and Gong [16].The combustion model from Micklow and Gong[16]makes considerable improvements in the predictions for in-cylinder pressure and heat release rate when compared with previous models, and also achieves good agreement between predicted soot NO(sub x)and measured values.

The simplest overall reaction representing the oxidation of a typical hydrocarbon fuel is one-step scheme,

$$\text{Fuel} + n_1O_2 \rightarrow n_2CO_2 + n_3H_2O \quad (1)$$

Where the stoichiometric coefficients $\{n_i\}$ are determined by the fuel. This global reaction is often a convenient way of approximating the effects of the many elementary reactions, which actually occur. Its rate must therefore represent an appropriate average of all the individual reaction rates involved. The single rate expression is usually expressed,

$$RR_{1\{chem\}} = AT^n exp(-E_a/RT)[fuel]^a[O_2]^b \quad (2)$$

Comparisons between computed and experimental combustion rates are required to evaluated the constants in the above equation, including the pre-exponential factor, A, the activation energy, E_a, n, a, and b. Note that, in general, a and b are not related to the stoichiometric coefficients in the global reaction, but are empirical constants determined either from experiment or from a detailed kinetics calculation [19].

Eq. (2) is based on chemical reaction rate, which may work well for premixed combustion. However, at the start of combustion only 10 to 35 percent of the vaporized fuel has mixed to within flammability limits in a typical medium speed DI diesel engine[20],[21], thus combustion is largely mixing-limited, especially in the late combustion stage. Such a non-premixed combustion may often be viewed as a mixing problem. Magnussen and Hjertager[22] proposed a model that relates the rate of combustion to the rate of dissipation of turbulent eddies and expressed the rate of reaction by the mean concentration of a reacting species, the turbulent kinetic energy and the rate of dissipation of this energy. In this model, the chemical reaction is assumed very fast and the rate of combustion will be determined by the rate of intermixing on a molecular scale of fuel and oxygen eddies. When excess oxidizer is present, the reaction rate is given by,

$$RR_{2\{lean\}} = C_A\overline{C_f}\left(\frac{\varepsilon}{k}\right) \tag{3}$$

when the fuel is in excess, the reaction rate is assumed to be,

$$RR_{3\{rich\}} = C_A\left(\overline{C_{O_2}}/r_f\right)(\varepsilon/k) \tag{4}$$

accounting for the burning rate in premixed turbulent flames, the reaction rate is,

$$RR_{4\{premix\}} = C_A C_B\left[\overline{C_p}/(1+r_f)\right](\varepsilon/k) \tag{5}$$

Where C_A,C_B are constants. C_A will depend on the structure of the flame and the rate of reaction between fuel and oxygen, and C_B is usually set empirically at 0.5. c_f, c_{O2}, c_p are ensemble averaged concentration of fuel, oxygen and products, respectively. ε is the rate of dissipation of turbulent kinetic energy, and k is the turbulent kinetic energy. r_f is the stoichiometric oxygen requirement to burn 1 kg fuel.

The equation that gives the lowest reaction rate in the eqns. (3)-(5) is the one that determines the local rate of combustion. Thus, an expression for the reaction rate is given by,

$$RR_{5\{local\}} = min(RR_{2\{lean\}}, RR_{3\{rich\}}, RR_{4\{premix\}}) \tag{6}$$

In the mixing-controlled combustion model, the chemical reaction rate is assumed very fast, which is not reasonable at the ignition delay stage of the combustion process due to low temperature. Although eq. (5) can account for this condition to some extent, the independence on chemistry of the mixing controlled model is one of its deficiencies. To overcome this shortcoming, eq. (2) is also considered when mixing-controlled model is employed in some applications. Further, numerous schemes can be generated in an attempt to model the physical phenomena. Several are as follows:

$$RR_6 = min(RR_{1\{chem\}}, RR_{2\{lean\}}, RR_{3\{rich\}}, RR_{4\{premix\}}) \tag{7}$$

$$RR_7 = max(RR_{1\{chem\}}, RR_{5\{local\}}) \tag{8}$$

$$RR_8 = min(RR_{1\{chem\}}, RR_{2\{lean\}}, RR_{3\{rich\}}) \tag{9}$$

Eq. (7) is typically not used as that it is likely to under predict the combustion rate, especially during the premixed combustion period. Eq. (8) is more reasonable in premixed combustion period, but may over predict the burning rate in the late stages of combustion. As $RR_{1\{chem\}}$ (eq. (2)) is able to account for the premixed combustion, $RR_{4\{premix\}}$ (eq. (5)) can be deleted in right hand of eq. (7) which results in eq. (9) In contrast to eq. (8), eq. (9) is more applicable for both the ignition delay and mixing controlled combustion stages. The combustion scheme given by eq. (9) is used in this study.

Four kinetic reactions and six equilibrium reactions were considered. They are as follows:

Kinetic reactions:

Fuel $+n_1O_2 = n_2CO_2 + n_3H_2O$

$O_2+2N_2 = 2N+2NO$

$2O_2+N_2 = 2O+2NO$ (10)

$2OH+N_2 = 2H+2NO$

Equilibrium reactions:

$H_2 \leftrightarrow 2H$

$O_2 \leftrightarrow 2O$

$N_2 \leftrightarrow 2N$

$O_2 + H_2 \leftrightarrow 2OH$ (11)

$O_2 + 2H_2O \leftrightarrow 4OH$

$O_2 + 2CO \leftrightarrow 2CO_2$

4. RESULTS AND DISCUSSION

This work investigates the effects of varying equivalence ratio, injector timing, and injection duration on emission and power production in a Caterpillar 3406 compression ignition engine. A total of 48 cases were investigated. This effort required over 500 computing hours on an IBM iDataplex system, comprised of 48 compute nodes (Total of 576 processor cores and 1,152GB RAM) and 1 head node.

A 360° mesh was generated rather that a 60° sector mesh to ensure a more accurate modeling of the in-cylinder flow structures. In earlier studies by Micklow and Gong [23] it was seen that important in-cylinder flow information related to tumble and swirl is lost when using a 60° sector mesh. A grid refinement study was performed to assure a grid independent solution. The grid is presented in Fig. The grid has 179,255 cells. Tablegives the engine operating parameters**.**

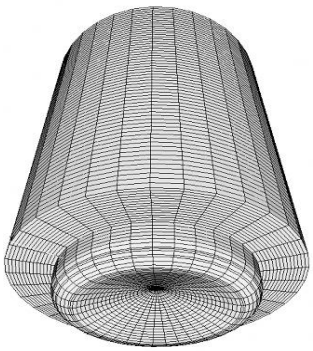

Fig2. *Cat 3406 mesh*

Table1. *Baseline engine specifications and operating conditions, equivalent to case# 18*

Bore*Stroke (mm):	137.6*165.1
RPM:	2200
Connect rod (mm):	261.62
Low limit for kinetic reaction calc:	800 K
Low limit for equilibrium chemistry calc.:	1200 K
Compression ratio:	15.1
Number of nozzle orifices:	6
Inlet air pressure:	240 kPa
Inlet temperature:	400 K
Injection pressure:	20.5 MPa
Fuel:	$C_{12}H_{26}$
Turbulence Model:	RNG
Cylinder wall temperature:	400 K
Cylinder head temperature:	525 K
Piston face temperature:	525 K
Crank angle BTDC to inject fuel:	31.5deg
Duration of injection pulse:	21.5deg
Displacement volume:	2.46L
Spray angle (deg from cylinder head):	27.5°
Global Equivalence Ratio:	0.4

Equivalence ratio is defined as the ratio of actual fuel to air ratio over the stoichiometric ratio. Global in-cylinder equivalence ratio is defined as the overall equivalence ratio for the entire cylinder volume, as opposed to local equivalence ratio which is defined as the equivalence ratio at some incremental volume in the cylinder. The global equivalence ratio is held fixed for all cases. For these studies, a baseline case is as described in Table and then effects of varying local equivalence ratio was investigated by varying injector timing, and injection duration for a 6 hole and 8 hole nozzle configuration. These cases are numerically labeled according to their execution order, for example Case 23 was the 23rd iteration in which changes were made. The details of these changes, relative to each case are listed in Table with the baseline parameters for the cases listed in Table.

Table2. *Variations between simulation cases*

Case #	Injection Start (degrees BTDC)	Injection Duration (degrees)	Number of Injector Holes
18	31.5	21.5	6
23	31.5	21.5	8
31	24.5	14.5	8
32	20.5	14.5	8
35	18.5	14.5	8
36	22.5	12.5	8
37	22.5	10.5	8
38	22.5	11.5	8
41	22.5	14.5	8
43	20	15	8
44	22.1	14.5	8
45	22.2	14.5	8
46	22.3	14.5	8
47	22.4	14.5	8
48	22.2	14.5	8

5. NO FORMATION

For the cases in this study the dominant form of NO production is thermal NO. An extended Zeldovich mechanism is used to model the formation. Reduction of total engine out NO production can be controlled with careful control of the in-cylinder formation:

- **Reducing combustion temperature**

Combustion temperature reduction can be accomplished by adjusting equivalence ratio. This technique can be accomplished by running either lean or rich air fuel mixtures.

- **Reducing residence time**

Reducing residence time at high temperatures can be done by ignition or injection timing with internal combustion engines. Short residence time at peak temperature keeps the vast majority of nitrogen from becoming ionized.

In a compression ignition engine, the fuel distribution is non-uniform and pollutant formation processes are strongly dependent on the localized vaporous fuel distributions and how those distributions change with time due to mixing. Figshows this non-uniform distribution on a cut plane across nozzle's plane for the 6 hole nozzle. The fuel droplets are colored by droplet velocity with red being the highest.

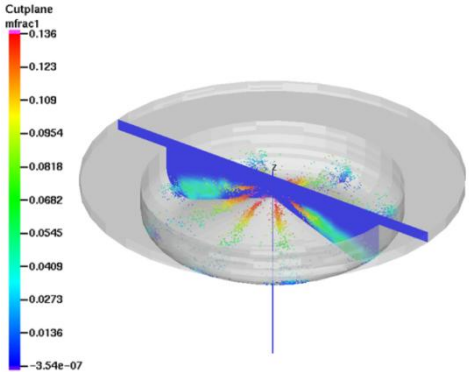

Fig3. *Mole fraction of vaporous fuel 7 degrees BTDC*

As indicated earlier reducing the maximum temperature or the residence time can reduce the amount of NO in the exhaust gases. Numerous cases were run with the six hole nozzle configuration. After comparing with an eight hole configuration, it was found that this configuration was clearly superior in performance. In-cylinder fuel distribution was improved thereby allowing better control of the vaporous fuel distribution or local equivalence ratio. This allowed a markedly improved control on NO formation. Therefore, the results presented here will concentrate on the eight hole configuration. Figshows marked difference for Cases 23 and 37. Case 23 used the same injection timing, duration and amount of fuel as Case 18 but two additional injection spray holes were added to the injector. These additional spray holes created a much more uniform fuel distribution which led to higher temperatures inside the cylinder producing a dramatic increase in NO. The difference in NO produced between Cases 18 and 23 served as one of the baseline data sets for the remainder of the studies.

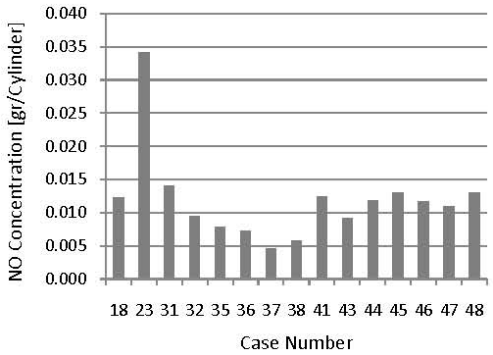

Fig4. *NO concentration versus crank shaft angle for cases varying local equivalence ratio*

Fig shows the maximum temperature inside the cylinder versus crank shaft angle for Cases 23 and 37.

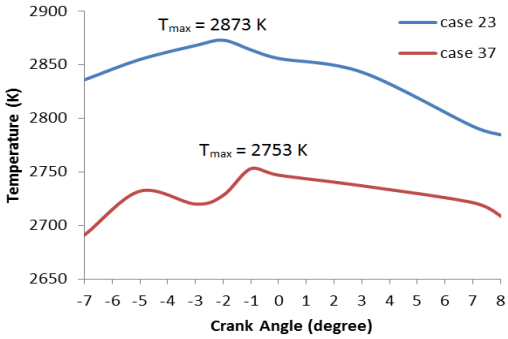

Fig5. *Maximum temperatures versus crank shaft angle*

The thermal NO formation rate is highly dependent on temperature; this strong dependency is evident in exponential term in eq. (12), where [Species] indicates a species concentration, and T indicates temperature in Kelvin.

$$\frac{d[NO]}{dt} = \frac{6\times10^{16}}{T^{0.5}} exp\left(\frac{-69000}{T}\right)[O_2]_e^{0.5}[N_2]_e \qquad (12)$$

The temperature difference and its effect on NO formation are shown in Fig and Fig.

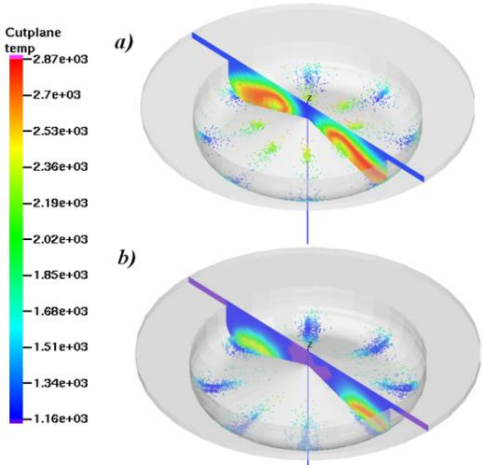

Fig6. *Temperature contour (K) for a) Case 23 (at 2°BTDC) and b) Case 37 (at 1° BTDC)*

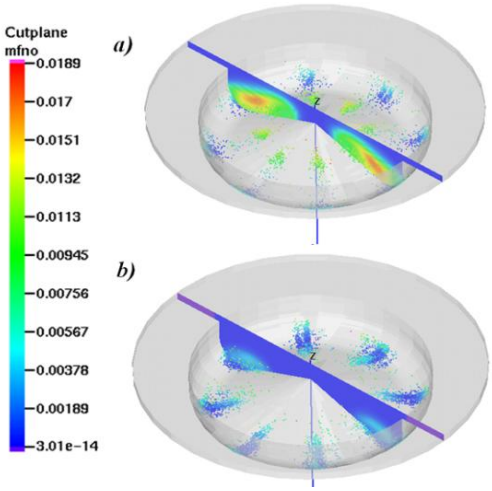

Fig7. *Mole fraction of NO contour for a) Case 23 (at 2°BTDC) and b) Case 37 (at 1° BTDC)*

In Fig and Fig it is clearly seen that the NO formation is higher in high temperature zones (initiation of ignition).

6. CHANGES IN LOCAL EQUIVALENCE RATIO

Variations in equivalence ratio on the local scale occur due to irregularities in the mixture homogeneity of fuel and air. These irregularities have several causes:

- Fuel injection spread pattern: The injection spray cone's angle of divergence and density distribution within that cone of spray directly affects local equivalence ratio gradients, with more uniform density distributions resulting in smoother gradient.
- Fuel penetration: Larger distances from the injector from which the fuel travels through the cylinder's gas volume can correlate to larger amounts of particle adhesion to wall and to other fuel particles. These irregularities result in sharp and persistent local equivalence ratio gradients.
- Fuel atomization and evaporation: Fuel evaporation and the dispersion of fuel resulting in smooth equivalence ratio gradients is desired and can be hindered by poor atomization and slow evaporation.
- Fuel particle collision and adhesion: Adhesion can result in larger local fuel concentrations as particles combine into larger fluid droplet volumes, which prevents rapid evaporation.

For more homogeneous local equivalence ratio gradients, burn rate becomes steadier and the minimum and maximums in equivalence ratio magnitude have less of an effect on engine performance and pollutant emission formation. Homogenizing the mixture composition, can avoid blowout at lower equivalence ratios. However, homogeneous local equivalence ratio gradients can also result in higher flame speeds which may induce knock and overpressure events.

Local equivalence ratio is used in this paper as a term to describe fuel distribution which is the only parameter which is varied in this study. Local equivalence ratio can be determined by looking at the fuel spray distribution directly which is done in the cases where the injector hole pattern is changed. Alternatively, since this paper is interested in determining if modifying the fuel distribution can effect pollutant emissions while maintaining engine performance, reaction behavior can be looked at directly in order to determine local equivalence ratio changes. This can be accomplished since more homogenous fuel distribution (smaller local equivalence ratio gradients) result in higher flame speeds, so flame speed can be used as an indicator of local equivalence ratio gradient uniformity.

Because flame speed is proportional to the simulations resulting Indicated Mean Effective Pressure (IMEP), relative changes between cases in IMEP are used as a comparison of fuel distribution homogeneity.

For the work in this paper, local equivalence ratio is modified using an iterative parametric study in which injection parameters are changed and trends are observed as a result of those changes. The first parameter examined is the injection pattern by increasing the number of fuel injector holes from 6 to

8. In simulation iterations conducted past case 23, the number of fuel injector holes is maintained at 8, while the injection start and duration are modified. In order to observe changes in local equivalence ratio for these later cases, the relative reaction distribution homogeneity can be focused on by monitoring the IMEP given by the PV diagrams in Fig for each case.

It can be observed that for the results seen in Table and Table, reduced local equivalence ratio gradients, i.e. more homogenous fuel distributions are indicated by a higher IMEP. The higher IMEP cases correlate to an increase in power and pollution formation, meaning that fuel distribution homogeneity approaching the global equivalence ratio of 0.4 throughout the chamber can have undesirable results. It then logically follows from the results shown that for some non-homogeneous propellant distribution shape; pollutant emissions can be decreased while maintaining engine performance such as in Cases 44 and 46 which are able to reduce the thermal efficiency difference to within 0.6% and -0.2% of the baseline case, which result in an -4.5% and a -3.1% reduction in the formation of NO respectively.

7. CAT 3406 INJECTION NOZZLE QUANTITY VARIATION

The baseline case was established for a global in-cylinder equivalence ratio of 0.4and verified to have good fuel penetration. This case, Case 18, with the standard 6 injection hole placement pattern show in Figa. The model was modified to increase the number of injection spray ports from 6 to 8 in an axisymmetric fashion, shown in Figb. Once this modification was complete, the model was run with the eight sprays and no parameter adjustments to verify fuel penetration and to determine what effect the fuel spray modification would have initially. This initial run which is labeled as Case 23 in this paper resulted in a 27% increase in thermal efficiency accompanied by 179% increase in NO production as seen in Fig.

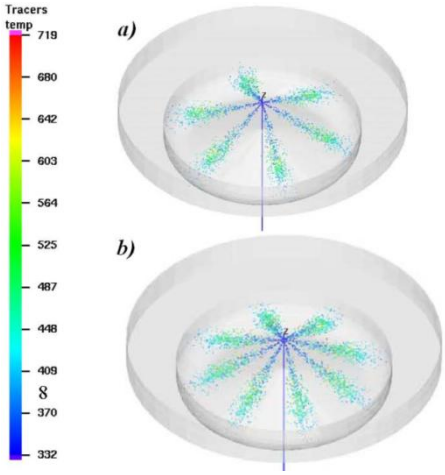

Fig8. *Injection pattern visualization by particle distribution and concentration: a) 6 injector pattern in Case 18, b) 8 injector pattern in Case 23.*

In Figb it can be seen that the fuel concentration becomes more evenly distributed and there are no longer isolated spots with increased concentration as indicated with the low velocity dark blue regions in Figa.

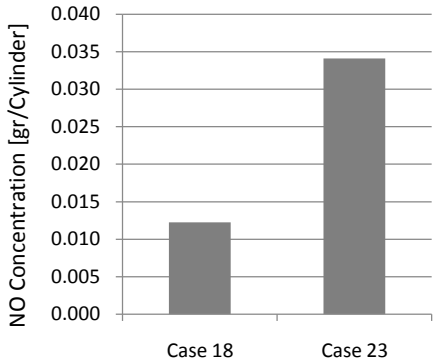

Fig9. *NO concentration verses crank angle for the baseline case (Case 18) using 6 nozzles, and the equivalence 8 nozzle case (Case 23)*

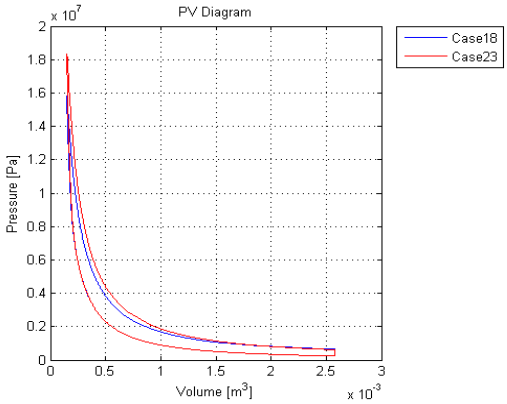

Fig10. *P-V diagram for the baseline case (Case 18) using 6 nozzles, and the equivalence 8 nozzle case (Case 23)*

With this increase in uniformity of fuel injection distribution, it is expected that burn rate will increase as well as power, and this is confirmed in Fig, where the area enclosed on the p-V diagram is significantly increased. With that increase in burn rate an increase in observed power increase resulted in increased NO pollutant emissions Fig**.**

8. INJECTION NOZZLE TIMING AND DURATION VARIATION

Through the adjustment of ignition timing and duration from the baseline case (Case 18) as well as using the 8 nozzle configuration, marked variations in product composition and thermal efficiency can be attained. The modified CAT 3406 cylinder with 8 nozzles is used for the trend study in this paper; the following parameters are varied to produce our case study: injection timing from -31.5 to -18.5 degrees BTDC, injection duration from 10.5 to 21.5 degrees of crank angle rotation, while equivalence ratio was held at 0.4 for all cases examined. The specifics for each change in parameter for each case, which are labeled sequentially according to when the case was computed, are listed on Table in the appendix, along with results of the global parameters, indicated power, IMEP, and thermal efficiency.

The 14 resulting combinations of cases from the parametric study are plotted as a function of crank angle in Fig through Fig.

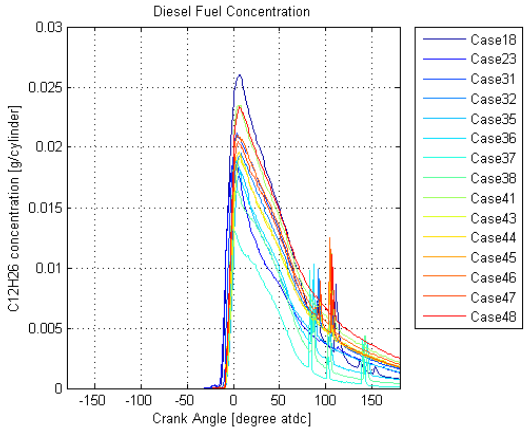

Fig11. *Local equivalence ratio parameter variation cases plotted for vaporous fuel (C12H26) concentration vs. crank angle (degrees)*

In Figit can be seen that for slower burn rate cases (Cases 35-38) the fuel evaporates and burns similarly to a slow diffusion flame, where the fuel droplets evaporate and combust, presenting only small amount of fuel vapor during this process, while the majority of the fuel volume is either in a liquid state or combusted. This is in contrast to the more homogeneous, higher burn rate results, which display more complete combustion with reduced secondary combustion events. In these cases, atomization and evaporation occurs faster and largely prior to ignition, resulting in a larger fuel vapor concentration in the plot as shown in Figfor the higher burn rate cases. The spikes in the figure are related to a late evaporation rate of the fuel associated with localized burning.

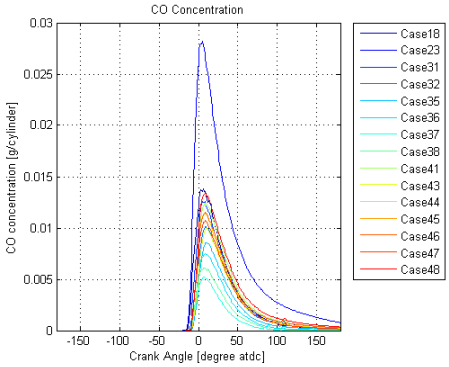

Fig12. *Local equivalence ratio parameter variation cases plotted for CO concentration vs. crank angle (degrees)*

In Fig, the CO concentration rate as well as magnitude can be resolved from the resulting cases. It can be seen that in Cases 35-38 the CO production occurs more slowly and a smaller maximum amount is formed; while in the alternate cases, the CO concentration production rate increases, correlating to a higher burn rate and a larger peak in CO emission magnitude. It can also be observed that while Case 18 was chosen as the baseline case for its large increase in burn rate, the deviation caused by variation of injection timing and duration which influence local equivalence ratio gradient, causes significant variation in CO production rate from -95% change from the baseline case (Case 18 toCase 37) to 615% change from the baseline case (Case 18 to Case 23). These increases in burn rates also correlate to higher thermal efficiencies as shown in Table.

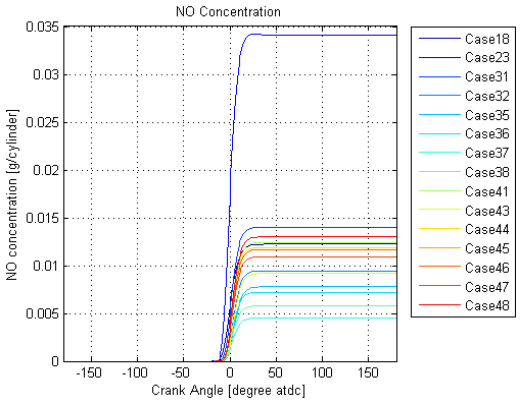

Fig13. *Local equivalence ratio parameter variation cases plotted for NO concentration vs. crank angle (degrees)*

In Fig NO formation trends are shown for all 15 cases including the baseline case, where the slower burn rates often predict lower NO formation, and yet some combinations of injection timing and duration, such as in cases 44 and 46, reveal decreases in NO can be observed while also displaying increases in burn rate shown in Fig and thermal efficiency as shown in Table. These optimum cases are discussed in further detail in the next section.

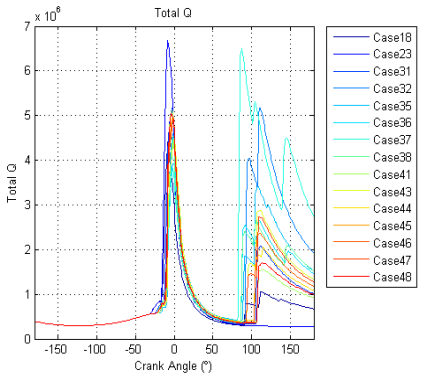

Fig14. *Local equivalence ratio parameter variation cases plotted for total Q (heat release in Joules) vs. crank angle (degrees)*

In the plot of total heat release (Q) vs. crank angle, Fig, it can be seen that for slower burn rates (Cases 35-38) the non-homogeneity of the fuel distribution caused by the sharpened equivalence ratio gradients results in increasingly larger secondary combustion events. Case 23 showcase the largest increase in thermal efficiency with a 27.2% increase from the baseline case, as well as being the only case to exhibit no secondary combustion events. This is thought to be due to the fact that fuel was injected earlier than all the other cases at -31.5 degrees ATDC and longer, for a longer duration of 21.5 degrees, which is the same as Case 18 (the baseline case), however with a more uniform fuel distribution caused by the increase in nozzle number from 6 to 8, this large effect in the combustion phenomenon can be observed.

In contrast with the high burn rate cases, Cases 35-38, the cases which resulted in the lowest burn rates, exhibit the highest number of secondary combustion events along with the largest decreases in power generation as shown in Tableand Fig.

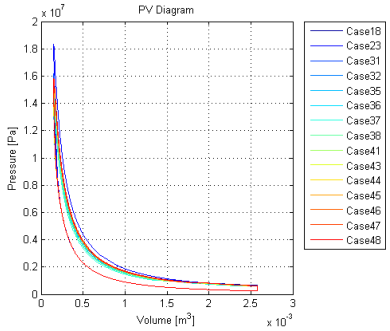

Fig15. *Local equivalence ratio parameter variation cases plotted for Pressure (Pa) vs. Volume (m^3)*

In Fig it can be observed that trends in flame speed and emissions also hold true for power generation, i.e. higher flame speeds, results in higher power outputs as seen from the P-V diagrams. A trend of early ignition start crank angle producing increases in power can also be observed, as shown in Table and Fig.

9. OBSERVED TRENDS FROM PARAMETRIC VARIATION

When varying injection timing and duration for the CAT 3406 engine to affect the uniformity of local equivalence ratio gradients, several trends are observed that may help to predict efficiency gains and emission reductions in future trials. For the 14 cases featuring 8-hole nozzles, where injection timing and duration were varied, a relation between injection starting time and emissions and efficiency was observed, as well as the parallel trends for injection duration. These trends are plotted in Fig through Fig where NO emissions, CO production rate, and thermal efficiency are compared against injection start angle.

Trends observed for injection start angle are observed to be as follows: In Fig a trend in NO formation can be seen to relate increasing injection start timing to a decrease in NO. In Figa trend in changing thermal efficiency vs. injection start timing is seen to relate an increase in injection start time to a decrease in thermal efficiency. In Fig, a trend in CO production rate vs. injection start timing. An increase in injection start time produces a decrease in CO production rate, and therefore burn rate.

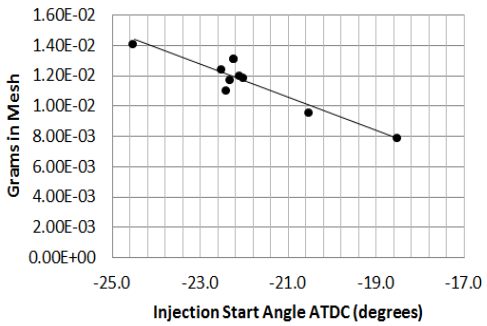

Fig16. *Trend in NO emission formation vs. injection start angle for local equivalence ratio variation case studies*

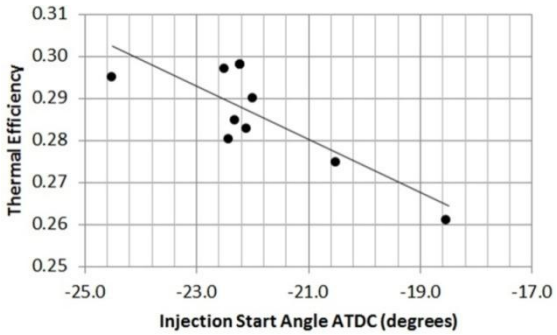

Fig17. *Trend in Thermal efficiency vs. injection start angle for local equivalence ratio variation case studies*

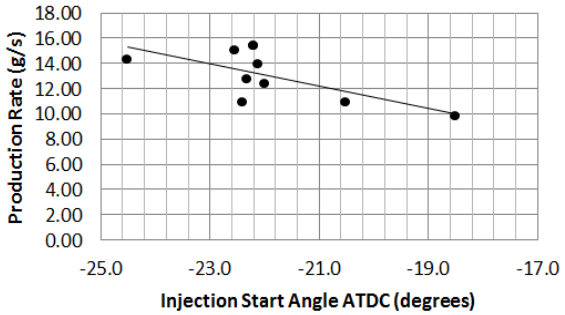

Fig18. *Trend in CO production rate in g/s vs. injection start angle for local equivalence ratio variation case studies*

From Fig, an increase in NO emissions as injection duration increases is shown. In Fig, thermal efficiency increases as injection duration increases. In Fig, CO production rate increases as injection duration increases. The clumps of points in Figthrough Fig signify a period of testing where the injection duration was held constant and the injection starting position was varied which can also be seen in Fig through Fig where the data points clump together. This uneven clumping of simulation parameters allowed for a higher resolution to be gained in the area where the NO reduction was observed to be the greatest while maintaining thermal efficiency.

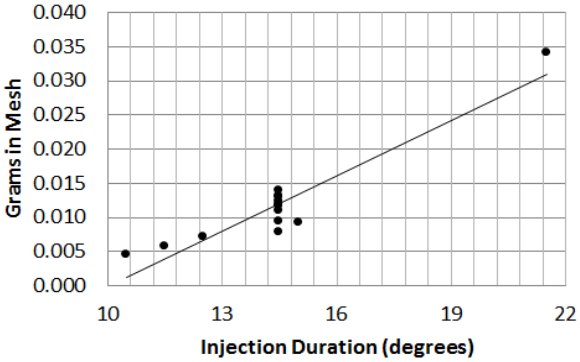

Fig19. *Trend in NO emission formation in grams vs. injection duration for local equivalence ratio variation case studies.*

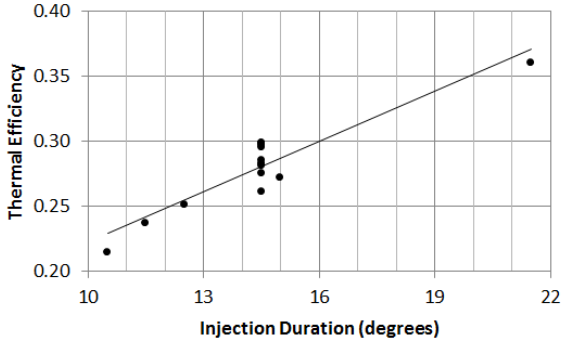

Fig20. *Trend in thermal efficiency vs. injection duration for local equivalence ratio variation case studies*

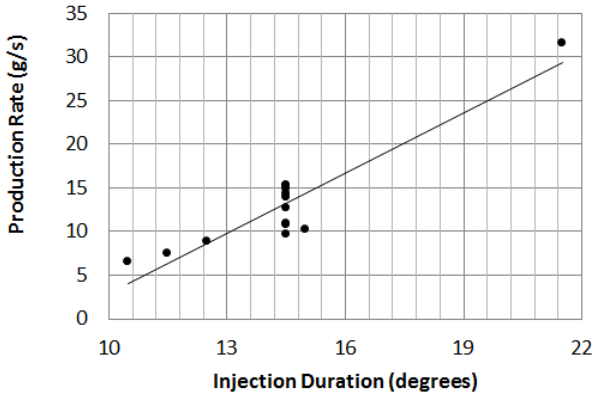

Fig21. *Trend in CO production rate vs. injection duration for local equivalence ratio variation case studies*

10. OPTIMIZED CASES

Through comparisons to the baseline case, i.e. case 18 it was shown in that an increase in injection nozzle number results in a more homogenous mixture of fuel and air, and increased power generation. However, with the increase in power generation, localized temperature increases caused an increase in NO production. However, from this increased power case, further optimization of local equivalence ratio gradients is shown make further improvements from the baseline case with the increased power and reduced emissions.

The tailoring of ignition timing and duration resulted in increased dispersion fuel injection patterns, with reductions in emissions while still maintaining power can be achieved using current technologies.

The most promising results from the 14 parameter variation cases were cases 44 and 46, in which the NO reduction occurred without significant power losses. In Case 44, ignition timing ATDC in degrees is -22.1 with injection duration of 14.5 degrees. While in Case 46, ignition timing ATDC in degrees is -22.3 with injection duration of also 14.5 degrees. In Fig, NO concentration for the baseline case (Case 18) with 6 fuel nozzles is compared to Cases 44 and 46 both with 8 fuel nozzles. A reduction in NO production is seen for cases 44 and 46.

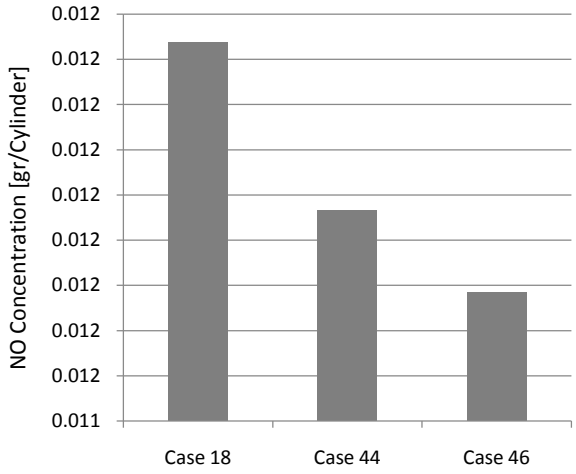

Fig22. *NO concentration vs. crank angle ATDC for the baseline case (Case 18) and the two optimum cases from the local equivalence ratio gradient case studies*

These optimal Cases 44 and 46 are able to reduce the thermal efficiency difference to within 0.6% and -0.2% of the baseline case, which result in an -4.5% and a -3.1% reduction in the formation of NO respectively as shown in Figand Table.This occurs when a ratio of injection starting in degrees ATDC to injection duration in degrees is about -1.5 where the injection duration is 14.5 degrees.

In Fig the P-V diagram for Cases 18, 44, and 46 are shown. The plots show that power generation is almost constant for all three cases.

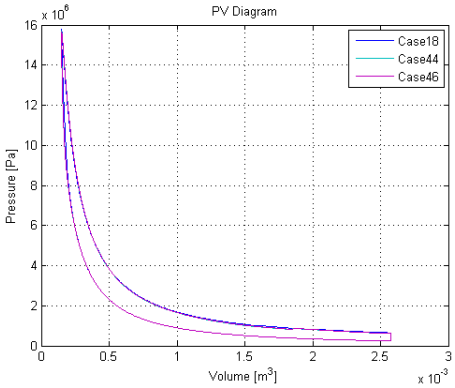

Fig23. *P-V diagram for the baseline case (Case 18) and the two optimum cases from the local equivalence ratio gradient case studies*

11. SUMMARY/CONCLUSIONS

In a closed combustion reactor, reactant distribution and composition play an important role in determining product formation and thermodynamic resultant properties. For applications to internal combustion engines, gains in thermodynamic efficiency and pollutant emission reduction is of paramount importance in the world today. By performing advanced simulations for engine combustion cycles, low cost research and development in engine technology can be realized. In this paper, the effect of equivalence ratio was investigated on both the local and global in-cylinder scales. Making use of trend recognition from literature that relates burn rate, product composition, and efficiency to the completed equivalence ratio variation procedure, a technical study of the effects and possible advances in engine performance was completed.

From the numerical simulations completed in this study, it can be shown that burn is a function of equivalence ratio. And that at close to homogeneous fuel and air mixtures, burn rate remains predictable and reduces such phenomena as secondary combustion events. While non-homogeneities in the mixture such as large local equivalence ratio gradient sizes can result in many combustion events, flame blowout, decreases in efficiency, and increases in pollutant emission formation.

This case which provides the highest burn rates is determined to be at a global equivalence ratio of 0.4. It is desired that a stable and uniform burn can be induced to occur at this lean end of the equivalence ratio range in order to produce the higher efficiencies, and lower pollutant emissions.

Then in the second portion of this work, a parametric study was compared to this 0.4 equivalence ratio optimum baseline case. From this study it is seen initial in-cylinder fuel distribution and mixture homogeneity is important from which it follows that modifying injector timing, duration, and nozzle number can result in in-cylinder variations to increase engine efficiency and power while continuing to reduce harmful emissions.

It is found that by increasing the number of fuel holes in the injector, mixture uniformity improves and power output increases. For the 0.4 global equivalence ratio, with the assumptions associated with this computational study for the 6 injector baseline case, it is shown that a currently technologically achievable increase in injector fuel holes from 6 to 8 increases thermal efficiency and power by 27% from the baseline case, and increases NO production by 178% when no other parameters are changed. It is believed that similar increases in actual engine performance could be obtained as in this computational study.

At the level of local equivalence ratio changes, modifications to the ignition process were made and it is found that an increase in injection duration causes an increase in CO production rate, flame speed, thermal efficiency, and NO emissions. It is also found that an increase in injection starting time correlates to a decrease to CO production rate, burn rate, thermal efficiency, and NO emissions for the range of injection timing run in this study. Using these trends, and KIVA3 to simulate new data points, it is found that while using the 8 injector case, current estimates show a 3-4% reduction in NO emissions can be produced when compared to the baseline case, while retaining an ability to preserve the baseline case's power and efficiency. From study, this paper concludes that through varying fuel injection start and duration and currently available cost effective technologies to produce nozzles with an increase in number of fuel injection holes, emissions can be reduced while still preserving or increasing power and efficiency.

REFERENCES

[1] National Research Council, 2001, "Review of the Research Program of the Partnership for a New Generation of Vehicles: Seventh Report," The National Academies Press, Washington, DC.

[2] Befrui, B., Corbinelli, G., D' Onofrio, M., and Varble, D., 2011, "GDI Multi-Hole Injector Internal Flow and Spray Analysis," SAE Technical Paper 2011-01-1211.

[3] Mathieu, O., Lavy, J., Jeudy, E., 2009, "Investigation of Hydrocarbons Conversion over a Pt-Based Automotive Diesel Oxidation Catalyst: Application to Exhaust Port Fuel Injection," DOI 10.1007/s11244-009-9365-3, Top Catal Springer Science + Business Media.

[4] Schrödinger, C., Paschereit, C.O., Oevermann, M., 2012, "Numerical studies on the impact of equivalence ratio oscillations on lean premixed flame characteristics and emissions," Presented at Seventh International Conference on Computational Fluid Dynamics, ICCFD7-3401.

[5] Azimov, U.B., Kim, K.S., Jeong, D.S., Lee, Y.G., 2009, "Evaluation of Low-Temperature Diesel Combustion Regimes with n-Heptane Fuel in a Constant-Volume Chamber," International Journal of Automotive Technology, 10(3).

[6] Dempsey, A., Walker, N., and Reitz, R., 2013, "Effect of Piston Bowl Geometry on Dual Fuel Reactivity Controlled Compression Ignition (RCCI) in a Light-Duty Engine Operated with Gasoline/Diesel and Methanol/Diesel," SAE Int. J. Engines 6(1), pp.78-100.

[7] Lilik, G., Boehman, A., 2013," Effects of Fuel Composition on Critical Equivalence Ratio for Autoignition", DOI: 10.1021/ref3016014, Energy & Fuels, 27 (3).

[8] Amsden, A. A., 1999,"KIVA-3V, Released 2, Improvements to Kiva-3v," Technical Report, LA-13608-MS, Los Alamos National Laboratory, Los Alamos, N. Mex., USA.

[9] Dukowitz, J. K., 1980, "A Particle-Fluid Numerical Model for Liquid Sprays," J. Comput. Phys., 35(229).

[10] O'Rouke, P. J., 2006, "Statistical Properties and Numerical Implementation of a Model for Droplet Dispersion in a Turbulent Gas," J. Comput. Phys., in press.

[11] O'Rourke, P. J., 1981, "Collective Drop Effects in Vaporizing Fuel Sprays," Ph.D. Thesis 1532-T, Princeton University.

[12] O'Rourke, P. J. and Amsden, A. A., 1989, "The TAB Method for the Numerical Calculation of Spray Droplet Breakup," SAE Technical Paper 872089.

[13] Corcione, A. L., Fusco, F. E., Papetti, A. and Succi, S., 1994, "Evaluation of Diesel Spray Breakup Models, Numerical Simulation and Experiments," ISASC, Hiroshima, Japan.

[14] Su, T. F., Patterson, M. A., Reitz, R. D. and Farrell, V., 1996, "Experimental and Numerical Studies of High Pressure Multiple Injection Sprays," SAE paper 960861.

[15] Micklow, G. J. and Gong, W., 2001, "Combustion Modeling for Direct Injection Diesel Engines," Proc. of the Inst. Of Mech. Engrs. Journal of Automotive Engineering, 215(D5), pp.651-662.

[16] Micklow, G. J. and Gong, W., 2002, "A Multi-Stage Combustion Model and Soot Formation Model for Direct-Injection Diesel Engines," Proc. of the Inst. Of Mech. Engrs. Journal of Automotive Engineering, 216(D), pp.495-504.

[17] Gong, W., 2001, "Combustion Modeling of Diesel and NG Fueled / Micro-pilot Diesel Ignition Engines," PhD dissertation, University of Alabama.

[18] Ayoub, N.S. and R.D. Reitz, 1995, "Multidimensional Computation of Multi-Component Spray Vaporization and Combustion", SAE paper 950285.

[19] Curtis, E.W., Uludogan, A., and R.D. Reitz, 1995, "A High Pressure Droplet Vaporization Model for Diesel Engine Modeling", SAE paper 952431.

[20] Taskinen, P., Karvinen, R. Liljenfeldt, G. and H.J. Salminen, 1996, "Simulation if Heavy Fuel Spray and Combustion in a Medium Speed Diesel Engine" SAE paper 962053.

[21] Uludogan, A., Foster, D.E. and R.D. Reitz, 1996, "Modeling the Effect of Engine Speed on the Combustion Process and Emissions in a DI Diesel Engine", SAE paper 962056.

[22] Magnussen, B. F., and B. H. Hjertager, 1977, "On Mathematical Models of Turbulent Combustion with Special Emphasis on Soot Formation and Combustion," Symposium (International) on Combustion 16(1), pp.719–729.

[23] Micklow, G.J. and W. Gong, 2008, "Investigation of the Grid and Intake Generated Tumble on the In-Cylinder Flow of a Direct Injection Compression Ignition Engine," Proceedings of the I MECH E Part D Journal of Automobile Engineering, Vol. 222, No. 5, pp. 775-788(14).

AUTHOR'S BIOGRAPHY

Gerald J. Micklow, PhD, PE, Professor, Department of Mechanical and Aerospace Engineering Head, Automotive Engineering, Director, Florida Center for Automotive Research, Florida Institute of Technology, 248 Olin Engineering Complex, Melbourne, FL 32901.

Annex A

Results Tables

Table3. *Local equivalence ratio parameter studies, tabulated results*

Case #	NO (grams)	NO % from baseline	CO (grams)	CO % from baseline	Thermal Efficiency	Thermal Efficiency % from baseline
18	1.22E-02	0.00%	1.05E-04	0.00%	0.2832	0.00%
23	3.41E-02	178.80%	7.51E-04	615.10%	0.3601	27.20%
31	1.40E-02	14.30%	1.89E-04	80.00%	0.295	4.20%
32	9.47E-03	-22.60%	1.59E-04	51.40%	0.2744	-3.10%
35	7.79E-03	-36.40%	1.02E-04	-2.80%	0.2608	-7.90%
36	7.23E-03	-40.90%	4.40E-05	-58.20%	0.2506	-11.50%
37	4.53E-03	-63.00%	4.64E-06	-95.60%	0.2141	-24.40%
38	5.82E-03	-52.40%	1.89E-05	-82.00%	0.2362	-16.60%
41	1.24E-02	1.50%	2.60E-04	147.60%	0.2969	4.80%
43	9.18E-03	-25.00%	1.73E-04	65.00%	0.2718	-4.00%
44	1.19E-02	-3.10%	1.96E-04	86.30%	0.2825	-0.20%
45	1.30E-02	6.20%	3.43E-04	226.90%	0.298	5.30%
46	1.17E-02	-4.50%	2.61E-04	148.50%	0.2848	0.60%
47	1.09E-02	-10.80%	1.66E-04	58.10%	0.2803	-1.00%
48	1.30E-02	6.20%	3.43E-04	226.90%	0.298	5.30%

Table4. *Local equivalence ratio parameter studies, tabulated results continued*

Case #	CO Production Rate (g/s)	CO Production Rate % from baseline	Indicated Mean Effective Pressure (kPa)	Indicated Mean Effective Pressure % from baseline	Indicated Power (kW)	Indicated Power % from baseline
18	10.46	0.00%	901.41	0.00%	40.31	0.00%
23	31.59	201.90%	1146.35	27.17%	51.27	27.17%
31	14.29	36.60%	939.05	4.18%	42	4.18%
32	10.91	4.20%	873.58	-3.09%	39.07	-3.09%
35	9.72	-7.10%	830.33	-7.89%	37.13	-7.89%
36	8.79	-16.00%	797.68	-11.51%	35.68	-11.51%
37	6.54	-37.50%	681.65	-24.38%	30.49	-24.38%
38	7.49	-28.40%	751.76	-16.60%	33.62	-16.60%
41	14.9	42.40%	945.07	4.84%	42.27	4.84%
43	10.15	-3.00%	865.2	-4.02%	38.69	-4.02%
44	13.86	32.50%	899.42	-0.22%	40.23	-0.22%
45	15.26	45.90%	948.77	5.25%	42.43	5.25%
46	12.66	21.00%	906.68	0.58%	40.55	0.58%
47	10.82	3.50%	892.34	-1.01%	39.91	-1.01%
48	15.26	45.90%	948.77	5.25%	42.43	5.25%